

1  
2  
3  
4  
5  
6  
7  
8  
9  
10  
11  
12  
13  
14  
15  
16  
17  
18  
19  
20  
21  
22  
23  
24

**Simulated coordinated impacts of the previous autumn NAO  
and winter El Niño on the winter aerosol concentrations over  
eastern China**

Juan Feng<sup>1</sup>, Jianping Li<sup>2,1</sup>, Hong Liao<sup>3</sup>, and Jianlei Zhu<sup>4</sup>

1. *College of Global Change and Earth System Science, Beijing Normal University, Beijing, China*

2. *Key Laboratory of Physical Oceanography–Institute for Advanced Ocean Studies, Ocean University of China and Qingdao National Laboratory for Marine Science and Technology, Qingdao 266003, China*

3. *School of Environmental Science and Engineering, Nanjing University of Information Science & Technology, Nanjing, China*

4. *China-ASEAN Environmental Cooperation Center, Beijing, China*

***Corresponding author:***

*Dr. Juan Feng*  
*College of Global Change and Earth System Science (GCESS),*  
*Beijing Normal University, Beijing 100875, China*  
Tel: 86-10-58802762  
Email: [fengjuan@bnu.edu.cn](mailto:fengjuan@bnu.edu.cn)

## Abstract

25

26 The high aerosol concentrations (AC) over eastern China have attracted attention from  
27 both science and society. Based on the simulations of a chemical transport model using  
28 a fixed emissions level, the possible role of the previous autumn North Atlantic  
29 Oscillation (NAO) combined with the simultaneous El Niño-South Oscillation (ENSO)  
30 on the boreal winter AC over eastern China is investigated. We find that the NAO only  
31 manifests its negative impacts on the AC during its negative phase over central China,  
32 and a significant positive influence on the distribution of AC is observed over south  
33 China only during the warm events of ENSO. The impact of the previous NAO on the  
34 AC occurs via an anomalous sea surface temperature tripole pattern by which a  
35 teleconnection wave train is induced that results in anomalous convergence over central  
36 China. In contrast, the occurrence of ENSO events may induce an anomalous shift in  
37 the western Pacific subtropical high and result in anomalous southwesterlies over south  
38 China. The anomalous circulations associated with a negative NAO and El Niño are not  
39 favorable for the transport of AC and correspond to worsening air conditions over  
40 central and south China. The results highlight that the combined effects of tropical and  
41 extratropical systems play considerable role in affecting the boreal winter AC over  
42 eastern China.

43

## 44 **1. Introduction**

45 Atmospheric particles (i.e., aerosols) are the key pollutants that exhibit an  
46 important adverse impact on human health, environmental pollution, global climate  
47 change, and atmospheric visibility (IPCC, 2013). Aerosol particles may alter the  
48 precipitation rates and optical properties of clouds (Hansen et al., 1997), impacting the  
49 radiation balance of the entire Earth-atmosphere system via absorbing and scattering  
50 solar radiation (Jiang et al., 2017; Yue and Unger, 2017). A better understanding of  
51 aerosol variations is therefore important and useful for scientific and social endeavors.

52 The meteorology parameters, i.e., atmospheric temperature (Aw and Kleeman,  
53 2003; Liao et al., 2015), boundary layer (Kleeman, 2008; Yang et al., 2016), wind (Zhu  
54 et al., 2012; Yang et al., 2014, 2017; Feng et al., 2017), and humidity (Ding and Liu,  
55 2014), show a non-negligible impact on the regional aerosol concentrations (AC) via  
56 affecting the deposition and transportation processes. Moreover, the intraseasonal and  
57 interannual variations in climatic phenomena could affect both the spatial and temporal  
58 accumulation and distribution of AC due to the associated variations in the circulation  
59 and rainfall anomalies. For example, the monsoon onset could affect the seasonal  
60 variations in regional AC (Tan et al., 1998; Chen and Yang, 2008). The interannual  
61 variation of AC over East Asia is connected with the interannual variation of East Asian  
62 winter monsoon (Jeong and Park, 2016; Lou et al., 2016, 2018; Mao et al., 2017) and  
63 summer monsoon (EASM; Zhang et al., 2010; Zhu et al., 2012). The seasonal evolution  
64 of the El Niño-South Oscillation (ENSO) impacts the seasonal variations of AC over  
65 northern and southern China (Liu et al., 2013; Feng et al., 2016a, 2017). The AC

66 variation in the US is influenced by the Pacific Decadal Oscillation (Singh and  
67 Palazoglu, 2012). These findings suggest that the role of climate systems in impacting  
68 the regional air quality cannot be ignored.

69 The North Atlantic Oscillation (NAO), reflecting large scale fluctuations in  
70 pressure between the subpolar low and subtropical high, is one of the most determinant  
71 and influential climate variability modes in the extratropical Atlantic Ocean, (e.g.,  
72 Hurrell, 1995; Gong et al., 2001; Visbeck et al., 2001). A negative (positive) polarity of  
73 the NAO is reflected by positive (negative) pressure anomalies over the high latitudes  
74 of the North Atlantic and negative (positive) pressure anomalies over the central North  
75 Atlantic. Both the positive and negative phases of NAO are accompanied with large  
76 scale modulations in the location and intensity of the North Atlantic jet stream and  
77 storm track (Gong et al., 2001; Li and Wang, 2003). The surface layer wind would vary  
78 associated with changes in the jet stream because of the NAO's quasi-barotropic  
79 characteristic, resulting in varied Ekman heat transport and basin-wide variations in the  
80 underlying sea surface temperatures (SST; Marshall et al., 2001; Wu et al., 2009; Wu  
81 and Wu, 2018).

82 The NAO massively impacts the temperature and precipitation patterns over the  
83 US and central Europe, i.e., a wet and warm winter in Europe, and mild and wet winter  
84 conditions would be expected accompanied with a positive NAO phase. Moreover, the  
85 NAO exhibits significant cross-seasonal impacts on the downstream regional climate.  
86 For example, it is reported that variation in boreal spring NAO influenced the  
87 subsequent intensity of the EASM from 1979-2006 (Wu et al., 2009). The linkage

88 between the EASM and NAO has been further explored but on the interdecadal scale  
89 (Wu and Lin, 2012; Wu et al., 2012; Zuo et al., 2013), and it is suggested that the  
90 preceding spring NAO dominated the relationship of the NAO-EASM more than the  
91 simultaneous summer NAO, similar result is seen in Zheng et al. (2016). Xu et al. (2013)  
92 presented that the previous boreal summer NAO significantly influenced the following  
93 September rainfall over central China. These studies highlight the important role of the  
94 NAO signal on the climate in East Asia, especially the cross-seasonal impacts, which  
95 are beneficial for seasonal forecasting.

96 In addition to the influence of the extratropics, the impact originating from the  
97 tropics is another important driver of the climate anomalies in China. As the most  
98 dominant interannual variability of the tropical air-sea coupled system, the El Niño-  
99 Southern Oscillation (ENSO) exhibits profound influences on the weather and climate  
100 around the world (e.g., Ropelewski and Halpert, 1987; Harrison and Larkin, 1998). The  
101 occurrence of ENSO phenomenon displays significant effects in impacting the global  
102 and regional oceanic and atmospheric anomalous patterns (e.g., Rasmusson and  
103 Carpenter, 1982; Trenberth, 1997). The seasonal climate variation in China is closely  
104 linked with the evolution of ENSO events. For example, increased rainfall is expected  
105 to be found over the Huai-he and Yangtze River valley, whereas less rainfall is seen  
106 over northern and southern China during the decaying summer of an El Niño event  
107 (Zhang et al., 1996, 1999; Ye and Wu, 2018). During the developing autumn of an El  
108 Niño event, enhanced rainfall would be expected over southern China due to the  
109 associated anomalous shift in the western Pacific subtropical high (WPSH). However,

110 without significant influence during the developing summer (Feng et al., 2016b).  
111 During the mature winter, both the warm and cold events show significant impacts on  
112 the temperature and rainfall anomalies over eastern China (Weng et al., 2009; Wu et al.,  
113 2011; Wu and Zhang, 2015; Li et al., 2019; Zhang et al., 2019a, 2019b).

114 As shown above, both the NAO and ENSO significantly impact the climate over  
115 China. China now suffering from relatively high aerosol loading, and this is commonly  
116 ascribed to the increased emissions connected with the speedy economic growth.  
117 However, as discussed above that the role of meteorological conditions in affecting the  
118 AC cannot be ignored. Accordingly, it is of interest to explore the possible impacts of  
119 the NAO and ENSO on the distributions of AC over China. The possible impacts of the  
120 NAO on the aerosol has been discussed by Moulin et al. (1997) and Jerez et al. (2013);  
121 however, they concentrated on its influences on the North Atlantic Ocean and Europe,  
122 respectively. Feng et al. (2016a) indicated the potential effects of El Niño on the AC  
123 over China, but with a focus on the seasonal evolution. Therefore, does the NAO exhibit  
124 significant impacts on the AC, and how the combination of the NAO and ENSO affect  
125 the distribution of AC over China, as both of them show important modulation of the  
126 climate over China.

127 The above discussions provide the main motivation of the present work. The  
128 conditions in boreal winter are discussed in the present work, as this time is  
129 corresponding to the heat supply season and the AC over China peak during this season.  
130 The coordinated role of the previous autumn (September to November, SON) NAO and  
131 the simultaneous ENSO is compared to that of the NAO alone, and also as well as the

132 involved physical mechanisms. The rest of this paper is arranged as follows. Model,  
133 datasets, and methodology employed are presented in Section 2. The possible impacts  
134 of the NAO and ENSO on the AC are explored in Section 3. Section 4 discusses the  
135 involved physical mechanism. Section 5 provides the discussion and conclusions.

## 136 **2. Datasets, simulations, and methodology**

### 137 **2.1 Datasets**

138 The input background meteorological variables of the GEOS-Chem model show  
139 high degree of uniformity with the current widely used reanalyses (e.g., Zhu et al., 2012;  
140 Yang et al., 2014). Here, the SLP in the National Centers for Environmental  
141 Prediction/National Center for Atmospheric Research (NCEP/NCAR) reanalysis  
142 (Kalnay et al., 1996) with a  $2.5^\circ$  latitude  $\times$   $2.5^\circ$  longitude resolution, and the UK  
143 Meteorological Office Hadley Centre's sea ice and SST datasets (HadISST; Rayner et  
144 al., 2003) with a  $1^\circ$  latitude  $\times$   $1^\circ$  longitude resolution are used to verify the reliability  
145 of the Goddard Earth Observing System, Version 4 (GEOS-4).

### 146 **2.2 GEOS-Chem simulations**

147 The influences of the NAO on the simulated AC over China are examined using a  
148 three-dimensional tropospheric chemistry model, i.e., GEOS-Chem (version 8.02.01;  
149 Bey et al., 2001). The model is driven by assimilated meteorological fields from the  
150 GEOS-4 of the NASA Global Modeling and Assimilation Office, with a  $2^\circ$  latitude  $\times$   
151  $2.5^\circ$  longitude resolution, and 30 hybrid vertical levels. This model contains a detailed  
152 coupled treatment of tropospheric ozone-NO<sub>x</sub>-hydrocarbon chemistry, as well as

153 aerosols and their precursors, containing nitrate, black carbon, sulfate, sea salt,  
154 ammonium, mineral dust, dust aerosols, and organic carbon (Bey et al., 2001; Liao et  
155 al., 2007). The aerosol dry and wet depositions follow Wesely (1989) and Liu et al.  
156 (2001), with details in Wang et al. (1998). According to Liao et al. (2007), the AC were  
157 defined as PM<sub>2.5</sub> as follows,

$$158 \quad [PM_{2.5}] = 1.37 \times [SO_4^{2-}] + 1.29 \times [NO_3^-] + [POA] + [BC] + [SOA] \quad (1)$$

159  $SO_4^{2-}$ ,  $NO_3^-$ , POA, BC, and SOA are the aerosols particles of sulfate, nitrate, primary  
160 organic aerosol, black carbon, and second organic aerosol, respectively. The sea salt  
161 aerosols and mineral dust are not considered for that measurements indicate that they  
162 are not the major aerosol species in the eastern China during winter (Xuan et al., 2000;  
163 Duan et al., 2006).

164 The anthropogenic emissions in the GEOS-Chem and experiment design are  
165 similar to Zhu et al. (2012), in which the biomass burning emissions and anthropogenic  
166 emissions are fixed at year 2005 level in the simulation. That is the observed variations  
167 in the distributions of AC as seen below was due to the variations in meteorological  
168 conditions associated with climate events. Due to the longevity of the GEOS-4 datasets,  
169 the period 1986-2006 is focused on. GEOS-Chem is a well-recognized atmospheric  
170 chemistry model and is widely utilized due to its capability to well characterize the  
171 seasonal, interannual, and decadal variations of pollutant aerosols in the East Asia and  
172 beyond (e.g., Zhu et al., 2012; Yang et al., 2014, 2016; Feng et al., 2017). The well  
173 performance and wide application of GEOS-Chem provide confidence for employing

174 the model to investigate the coordinated impacts of NAO and El Niño on the AC over  
 175 eastern China.

### 176 **2.3 NAO index and Niño3 index**

177 The NAO index (NAOI) is employed to quantify the variations in the NAO phase  
 178 (Hurrell et al., 1995; Gong and Wang, 2001). The definition of the NAOI follows Li and  
 179 Wang (2003) and is calculated as the zonal mean SLP difference between 35°N (i.e.,  
 180 refers to the mid-latitude center) and 65°N (i.e., refers to the high latitude center) from  
 181 80°W to 30°E over the North Atlantic by

$$182 \quad \text{NAOI} = \hat{P}_{35^{\circ}\text{N}} - \hat{P}_{65^{\circ}\text{N}} \quad (2)$$

183 where  $P$  is the monthly mean SLP averaged from 80°W to 30°E,  $\hat{P}$  is the normalized  
 184 value of  $P$ , and the subscripts indicate latitudes. For a given month  $m$  in year  $n$ , the  
 185 normalization  $\hat{P}$  is defined as follows

$$186 \quad \hat{P}_{n,m} = \frac{P'_{n,m}}{S_P} \quad (3)$$

187 where  $P'_{n,m}$  is the monthly pressure anomaly of  $P_{n,m}$ , departure from period 1986-  
 188 2006, and  $S_P$  is the total standard deviation of the monthly anomaly  $P'_{n,m}$ ,

$$189 \quad S_P = \sqrt{\frac{1}{12 \times 21} \sum_{i=1986}^{2006} \sum_{j=1}^{12} P'_{j,i}{}^2} \quad (4)$$

190 The monthly NAOI is calculated based on the monthly mean SLP from both the  
 191 NCEP/NCAR and GEOS-4 assimilated meteorological dataset for 1986-2006. The  
 192 boreal autumn NAOI is defined as the average of the monthly NAOI during September,  
 193 October, and November (Fig. 1). The series of NAOI show strong interannual variations,

194 and the two series based on GEOS-4 and NCEP/NCAR are closely correlated with each  
195 other with a significant coefficient of 0.98, implying the GEOS-4 dataset could capture  
196 the variation in the NAO.

197 El Niño events were defined as standardized 3-month running mean Niño3 index  
198 (areal mean SST averaged over 150°-90°W, 5°N-5°S) above 0.5°C and persisting for at  
199 least 6 months. The skin temperature (i.e., SST over ocean and surface air temperature  
200 on land) was employed to obtain the Niño3 index for that SST is not available in the  
201 GEOS-4 meteorological dataset. The boreal winter Niño3 index is calculated as the  
202 average of the monthly Niño3 during December, January, and February, i.e., winter  
203 1997 is for the December 1997 and January and February 1998. The boreal winter  
204 Niño3 indices based on the GEOS-4 and HadISST are significantly correlated with each  
205 other, (Fig. 1), with a coefficient of 0.99. The high correlations among the indices  
206 further indicate the reliability of the model data.

### 207 **3. Influences of the NAO and El Niño on the AC over China**

#### 208 **3.1 Climatological Characteristics of the AC**

209 The spatial distribution of the standard deviation of boreal winter AC is shown in  
210 Fig. 2. Eastern China (105°E eastward, 35°N southward) shows high loading of  
211 aerosols in both the column and surface layer concentrations (figure not shown). Further,  
212 the variance of winter AC over eastern China is most pronounced compared to other  
213 regions during this season (Fig. 2a, b). As an evident monsoonal region, eastern Asia is  
214 influenced by winter monsoon, i.e., a strong Aleutian low is seen in the north Pacific,

215 and the Asian continent is controlled by the Siberian high during boreal winter. The  
216 strong pressure gradient between the Siberian high and Aleutian low results in strong  
217 northwesterlies prevailing over eastern China (Fig. 2c).

### 218 **3.2 Relationships between the AC & NAO and El Niño**

219 The spatial distribution between the surface AC and previous autumn NAOI and  
220 simultaneous winter Niño3 index are presented in Fig. 3. Positive correlations are seen  
221 over south (30°N south) and northwest China in the correlations with the Niño3 index,  
222 indicating that a warm ENSO event would associate with high AC over south and  
223 northwest China. In contrast, negative correlations over south and central China are  
224 observed in the correlations with autumn NAO, implying a positive NAO phase is  
225 linked with less AC over these regions, thus favoring better air conditions. The analysis  
226 suggests that the ENSO and NAO show opposite effects on AC over south China, i.e.,  
227 the NAO displays a negative impact and the ENSO displays a positive impact. However,  
228 the relationship between the autumn NAOI and winter Niño3 index is insignificant with  
229 a correlation of -0.08 during period 1986-2006.

230 The above relationships are further examined in their positive and negative phases,  
231 as strong asymmetry was reported in the climatic impacts of the NAO (Xu et al., 2013;  
232 Zhang et al., 2015) and ENSO (Cai and Cowan, 2009; Karior et al., 2013; Feng et al.,  
233 2016b). The asymmetric influences of the NAO and ENSO on AC are obvious in the  
234 spatial distributions of the linear correlation coefficients (Fig. 4). During the El Niño  
235 events, south China is impacted by significant positive correlations, in contrast, a non-

236 significant correlation is observed over this region during the La Niña events. This point  
237 implies the significant relationships between the ENSO and AC over south China are  
238 mainly connected with warm events, i.e., El Niño. The negative correlations between  
239 the NAO and AC mainly occurred in the negative phase of the NAO, and the significant  
240 correlations are mainly located in central China (lie from 28°N to 40°N). Thus, the  
241 ENSO affects the distribution of AC in south China, but the impact is manifested during  
242 warm events. Similarly, the effect of the NAO on the distribution of AC over central  
243 China is only apparent during its negative phase.

244 The results suggest that if the occurrence of a negative polarity of NAO overlaps  
245 with an El Niño event, the combined effects of the two may further worsen the AC over  
246 eastern China. In contrast, a solo occurrence of a negative NAO event is associated with  
247 above-normal AC over central China. The statistic significant impacts of the negative  
248 NAO and El Niño events on the AC could be further established by case study. Two  
249 cases, i.e., the co-occurrence of an El Niño event and a negative NAO, and a solo  
250 negative NAO event, were chosen to further explore the effect of the NAO and El Niño  
251 on the AC over China. From 1986-2006, there are two years (1997 and 2002) with  
252 equivalent negative values of autumn NAOI (-1.507 in 1997, and -1.510 in 2002).  
253 Winter 1997 corresponds with the strongest El Niño in the past 120 years and winter  
254 2002 corresponds with a neutral ENSO event. Consequently, the anomalous distribution  
255 of AC during these two years are discussed in the context of comparing the combined  
256 and solo effects of a negative NAO and El Niño in impacting the distribution of AC  
257 over eastern China.

### 258 **3.3 Influences of the NAO & El Niño vs. the NAO on the AC**

259 Figure 5 presents the layer and column AC anomalies simulated for the winters of  
260 1997 and 2002 departure from the climatological mean. Under the combined influence  
261 of a negative NAO and El Niño (1997), positive aerosol concentration anomalies are  
262 observed over eastern China (Fig. 5a, c). In addition, simulated enhanced AC were  
263 observed over central China in winter 2002 under the impacts of a negative NAO (Fig.  
264 5b, d). These characteristics are also apparent in the vertical distribution (Fig. 6), which  
265 shows the zonal mean anomalies averaged over eastern China ( $105^{\circ}$ – $120^{\circ}$ E). For winter  
266 1997, increased AC cover the whole eastern China, with maximum values  
267 approximately  $30^{\circ}$ N, where the effects of the NAO and El Niño overlap (Figs. 4a, d).  
268 The combined effects of the anomalies show a consistent distribution in the vertical  
269 levels (Fig. 6). In contrast, evident increased AC anomalies are seen in central China,  
270 with the maximum at approximately  $32^{\circ}$ N during winter 2002.

271 The consistent results between the correlations and anomalies during the two cases  
272 highlight the role of the negative NAO and El Niño events in determining the  
273 distribution of AC over eastern China. The NAO shows a significant influence on the  
274 central China AC that are only apparent during its negative phase, and the ENSO  
275 impacts the AC over south China mainly during warm events.

## 276 **4. Mechanisms of the effects of the NAO and El Niño on the AC**

### 277 **4.1 Role of circulation transport**

278 The corresponding reverse role of the NAO and El Niño in impacting the  
279 distribution of AC is mainly derived from their contrasting effects on circulation. Figure  
280 7 shows the SLP and surface wind anomalies during the autumns of 1997 and 2002,  
281 presenting an anomalously weak autumn NAO pattern. The negative phase of the NAO  
282 displays as an anomalous SLP dipole structure between the middle latitude North  
283 Atlantic Ocean and Arctic, i.e., with positive SLP anomalies at the Arctic over the  
284 Atlantic sector, and anomalous negative SLP at middle latitude. Although the locations  
285 of the anomalous pressure centers in the two negative NAO events show difference, the  
286 anomalous SLP amplitude in the two events are similar, i.e., with greater negative SLP  
287 anomalies at mid-latitudes, indicating that the pressure gradient of the two NAO  
288 negative events is similar. The oscillation in the SLP is connected with anomalies in the  
289 surface wind across the North Atlantic, i.e., associated with an anomalous cyclonic  
290 centered approximately 45°N and anti-cyclonic circulation anomalies around Iceland.  
291 During boreal winter and spring, an anomalous NAO could result in a tripole SST  
292 anomalous pattern in the North Atlantic Ocean (Watanabe et al., 1999). A similar SST  
293 tripole pattern is observed during boreal autumn, with warm SST anomalies at high and  
294 low latitudes, and negative SST anomalies at middle latitudes in the North Atlantic  
295 sector (Fig. 8a, c). Note that the negative SST anomalies during 1997 displays an east-  
296 west direction but originated from a northwest-southeast direction during 2002 due to  
297 the different locations of anomalous SLP (Fig. 7).

298 The North Atlantic anomalous SST tripole pattern is due to the feedback between  
299 wind-SST, i.e., the anomalous anti-cyclonic (cyclonic) circulation weaken (strengthens)

300 the prevailing westerlies, which would result in decreased (increased) loss of heat and  
301 warmer (cooler) anomalies in Ekman heat transport (Xie, 2004; Wu et al., 2009), and  
302 is connected to warmer (cooler) local SST. Due to the short memory of the atmosphere,  
303 the cross-seasonal influences of the NAO on the AC should be preserved in the  
304 boundary layer forcing such as SST (Charney and Shukla, 1981). This anomalous  
305 tripole SST pattern could persist to the following winter (Fig. 8b, d), as the anomalous  
306 tripole SST pattern during winter and autumn show high consistencies in both 1997 and  
307 2002, with significant spatial correlation coefficients of 0.32 and 0.51 between the  
308 autumn and winter tripole SST patterns for 1997 and 2002, respectively.

309 Figure 9 shows the anomalous divergence at the upper troposphere. The  
310 occurrence of a negative NAO phase is accompanied by an anomalous teleconnection  
311 wave train over northern Eurasia (AEA) in the upper troposphere during boreal summer  
312 (Li and Ruan, 2018). This anomalous teleconnection pattern is also observed during  
313 boreal winter, with a shift in the precise locations. Under the influence of the anomalous  
314 downstream teleconnection, north China is influenced by convergence anomalies, with  
315 the center positioned over central China (Fig. 9). The anomalous convergence is clearly  
316 seen in both the upper and lower troposphere, accompanied by anomalous easterlies or  
317 southeasterlies over central China (Fig. 10). The direction of the anomalous wind is  
318 opposite to the climatological winds, which would weaken the climatological wind and  
319 is unfavorable for the transport of aerosol concentration, leading to increased AC over  
320 central China, as displayed in Fig. 5.

321 For the winter 1997, corresponding to the El Niño's mature phase, south China  
322 was influenced by an evident anomalous divergence at the lower troposphere,  
323 indicating anomalous anticyclonic circulation over the coastal regions (Fig. 10a).  
324 Anomalous southwesterlies prevailed in south China, implying weakened northerlies.  
325 That is the anomalous meteorological conditions are unfavorable for aerosols transport  
326 in the region and would result in a worsen air quality. In contrast, for the winter 2002,  
327 south China was controlled by an anomalous divergence for that the main body of the  
328 WPSH shifts to the south of south China (Fig. 10b). The anomalous circulation was  
329 favorable for the emission of pollutant. Moreover, an evident anomalous divergence  
330 was observed in south China in the winters of 1997 and 2002 at the upper troposphere;  
331 however, the corresponding distribution of AC over this region is different. This  
332 highlights the role of El Niño in impacting the circulation anomalies over south China,  
333 as mentioned above. The occurrence of El Niño events would be accompanied by a  
334 northwest shift of the WPSH during boreal winter and enhanced southwesterlies over  
335 south China (Weng et al., 2009). Besides, column AC are mainly contributed by  
336 concentrations at lower troposphere, suggesting that the lower troposphere circulation  
337 may play a vital role in impacting the AC over south China.

#### 338 **4.2 Role of wet deposit**

339 In addition to the contribution of the circulation anomalies to the distribution of  
340 AC, changes in wet deposit also could affect distribution of AC. Figure 11 presents the  
341 simulated wet deposit anomalies during the winters of 1997 and 2002. Negative  
342 anomalies occurred over eastern China during the winter of 1997, favorable for

343 increased AC. This suggests the wet deposit plays a positive role in the enhanced AC  
344 during winter 1997. Positive anomalies were observed over central China in the 2002  
345 winter, inconsistent with the AC anomalies. The anomalous wet deposit during winter  
346 of 1997 is paralleling to the AC anomalies over eastern China; however, not consistent  
347 with that for the winter of 2002. This suggests that role of wet deposit in impacting the  
348 AC over eastern China exists uncertainties, showing strong regional dependence. The  
349 impact of wet deposit on the AC was examined by a sensitive experiment by turning  
350 off the wet deposition (Fig. 11c-d). A similar anomalous AC distribution was observed  
351 as those shown in Fig. 5, confirming that the role of wet deposit in impacting the  
352 distribution of AC is not as important as the circulation.

## 353 **5. Summary and Discussion**

354 Using the simulations of GEOS-Chem model with fixed emissions, the  
355 coordinated impacts of the previous autumn NAO and simultaneous ENSO on the  
356 boreal winter AC over eastern China are investigated. The results present that both the  
357 NAO and ENSO show asymmetry impacts on the boreal winter AC over eastern China,  
358 i.e., the NAO manifests negative impacts over central China during its negative phase  
359 and the ENSO positively impacts the AC over south China significantly during its warm  
360 events. Consequently, the possible impacts of two cases were investigated to ascertain  
361 the role of the NAO and ENSO on the distribution of AC over China. The winter 1997  
362 had a co-occurrence of a negative NAO and an El Niño events, and winter 2002  
363 corresponds to a negative NAO phase and neutral ENSO. For the winter 1997, obvious  
364 enhanced AC were observed over eastern China, with a maximum approximately 30°N,

365 where the impacts of the NAO and El Niño overlap. For the winter 2002, there were  
366 generally increased AC over central China. These results suggest that the co-occurrence  
367 of a negative NAO and El Niño would worsen the air conditions over eastern China,  
368 and a solo negative NAO is associated with increased AC over central China.

369 The cross-seasonal impacts of the preceding autumn NAO on the following winter  
370 AC over China can be explained by the coupled air-sea bridge theory (Li and Ruan,  
371 2018). The preceding negative NAO exhibits significant influences on the winds due to  
372 the adjustment of the wind to the anomalous SLP. The associated anomalous wind could  
373 affect the underlying regional SST, resulting in an anomalous SST tripole pattern over  
374 the North Atlantic. Since the North Atlantic SST exhibit strong persistence, this  
375 anomalous SST pattern could persist to the subsequent winter and inducing an  
376 anomalous AEA teleconnection wave train in the upper troposphere, with anomalous  
377 convergence over central China. Thus, central China is controlled by anomalous  
378 southeasterlies or easterlies, which weaken the climatological northwesterlies and  
379 induce increased AC over central China. In contrast, the occurrence of El Niño is linked  
380 to warm SST anomalies over tropical eastern Pacific, by which the Rossby wave  
381 activity would be altered (Wang et al., 2001; Feng and Li, 2011). A northwest shift of  
382 the WPSH is seen during the winter of an El Niño event, associated with southwesterlies  
383 anomalies over south China during the winter of 1997, indicating a weakening in the  
384 climatological wind and leading to in enhanced AC over south China. Therefore, the  
385 high level of AC over eastern China during the winter 1997 results from the combined

386 role of the NAO and El Niño, and the high concentrations over central China in the  
387 winter of 2002 are attributed to the NAO.

388 The possible reason for the asymmetric influence of the NAO on the AC was  
389 further explored. When the autumn NAO is in the positive polarity, for example, two  
390 positive cases of 1986 and 1992, the associated underlying SST anomalies (figure not  
391 shown), particularly the tripole SST pattern, are not as evident as those shown in the  
392 negative NAO. This result may provide a possible explanation for the asymmetric  
393 relationship existed in the different phases of the NAO and AC, and implies the  
394 complexity of the atmosphere-ocean feedback in the North Atlantic. This merits further  
395 exploration related to why the linkage between the NAO and underlying SST is  
396 nonlinear, and what process is responsible for their nonlinear relationship.

397 As noted above, the influence of the NAO on the AC only manifests during its  
398 negative phase, and the impact of the ENSO is only significant during its warm events.  
399 However, the relationship between the previous autumn and following winter ENSO is  
400 insignificant, thus it is of interest to establish the nonlinear relationship among them  
401 and investigate why there is strong asymmetry in the relationships. Zhang et al. (2015,  
402 2019) explored the complex linkage between the boreal winter NAO and ENSO with  
403 the former lagged for one month, indicating that the nonlinear relationship of the NAO  
404 and ENSO is modulated by the interdecadal variation in the Atlantic Multi-Decadal  
405 Oscillation. In addition, Wu et al. (2009) have illustrated the coordinated impacts of the  
406 NAO and ENSO in modulating the interannual variation of the EASM; however, it has  
407 not been shown to determine the AC yet. Therefore, it is of interest to further explore

408 whether the NAO and ENSO affect the AC over China in other seasons, as well as the  
409 process involved. Furthermore, the present work is based on model simulations and due  
410 to the limitations of the model simulations, only the interannual variations are  
411 considered. As both NAO and ENSO show strong interdecadal variations, for a longer  
412 period, i.e., 1850-2017 (figure not shown), the NAO during period 1986-2006 is  
413 generally located in the positive phase, whereas in the negative phase during period  
414 1955-1970, therefore, it is important to determine the interdecadal modulation of the  
415 NAO on the distribution of AC.

416 Moreover, the role of rainfall in influencing the AC shows uncertainties, i.e., a  
417 positive effect over south China but not for central China. This result is similar with  
418 that of Wu (2014), showing the impact of wet deposit on the AC shows regional and  
419 seasonal dependence. This is may due to the fact that the climatological winter rainfall  
420 over central China is much less than that over south China (figure not shown). In  
421 addition, the meteorological backgrounds of south China and central China are different,  
422 baroclinic over central China and barotropic over south China (Fig. 9 vs. 10), indicating  
423 the importance of climatology background in impacting the spatial distribution of AC.  
424 In addition, both the NAO and ENSO show significant correlations with AC over  
425 northwest China (Fig. 4); however, the interannual variation (Fig. 2) and anomalies (Fig.  
426 5) in AC over those regions are relatively small. Therefore, the AC variation over those  
427 regions are not discussed.

428 Finally, the role of NAO and El Niño on the AC during boreal winter was  
429 investigated based on GEOS-Chem simulations. The coordinated role of the NAO and

430 El Niño in affecting the distribution of AC over eastern China is highlighted by  
431 comparing this effect with the solo role of the NAO. The result indicates that the  
432 influence of meteorological factors impacting AC is complicated. Future work will  
433 investigate the combined role of tropical and extratropical signals on seasonal AC to  
434 better understand the variation across seasons and to determine the possible  
435 contribution of natural variability to the current aerosol loading over China.  
436

437 ***Author contribution***

438 J. F., J. L., and H. L. designed the research. J. F. and J. Z. performed the data  
439 analysis and simulations. J. F. led the writing and prepared all figures. All the authors  
440 discussed the results and commented on the manuscript.

441 ***Data availability***

442 Modeling results are available upon request to the corresponding author  
443 ([fengjuan@bnu.edu.cn](mailto:fengjuan@bnu.edu.cn)).

444 ***Acknowledgement***

445 This work was jointly supported by the National Natural Science Foundation of  
446 China (41790474, 41705131, and 41530424).

447

## References

448

449 Aw, J., and Kleeman, M. J.: Evaluating the first-order effect of intra-annual temperature  
450 variability on urban air pollution, *J. Geophys. Res. Atmos.*, 108, D12, 4365,  
451 <https://doi.org/10.1029/2002JD002688>, 2003.

452 Bey, I., Jacob, D. J., Yantosca, R. M., Logan, J. A., Field, B. D., Fiore, A. M., Li, Q. B.,  
453 Liu, H. Y., Mickley, L. J., and Schultz, M. G.: Global modeling of tropospheric  
454 chemistry with assimilated meteorology: Model description and evaluation, *J.*  
455 *Geophys. Res.*, 106, 23073-23095, <https://doi.org/10.1029/2001JD000807>, 2001.

456 Cai, W. J., and Cowan, T.: La Niña Modoki impacts Australia autumn rainfall variability,  
457 *Geophys. Res. Lett.*, 36, L12805, <https://doi.org/10.1029/2009GL037885>, 2009.

458 Chen, B. Q., and Yang Y. M.: Remote sensing of the spatio-temporal pattern of aerosol  
459 over Taiwan Strait and its adjacent sea areas, *Acta Scientiae Circumstantiae*, 28, 12,  
460 2597-2604, 2008.

461 Duan, F. K., He, K. B., Ma, Y. L., Yang, F. M., Yu, X. C., Cadle, S. H., Chan, T., and  
462 Mulawa, P. A.: Concentration and chemical characteristics of PM<sub>2.5</sub> in Beijing,  
463 China: 2001-2002, *Sci. Total Environ.*, 355, 264–275,  
464 <https://doi.org/10.1016/j.scitotenv.2005.03.001>, 2006.

465 Feng, J., and Li, J. P.: Influence of El Niño Modoki on spring rainfall over south China,  
466 *J. Geophys. Res. Atmos.*, 116, D13102, <https://doi.org/10.1029/2010JD015160>,  
467 2011.

468 Feng, J., Zhu, J. L., and Li, Y.: Influences of El Niño on aerosol concentrations over  
469 eastern China, *Atmos. Sci. Lett.*, 17, 422-430, <https://doi.org/10.1002/asl.674>,

470 2016a.

471 Feng, J., Li, J. P., Zheng, F., Xie, F., and Sun, C.: Contrasting impacts of developing  
472 phases of two types of El Niño on southern China rainfall, *J. Meteorol. Soc. Jap.*,  
473 94, 359-370, <https://doi.org/10.2151/jmsj.2016-019>, 2016b.

474 Feng, J., Li, J. P., J. Zhu, J. L., Liao, H., and Yang, Y.: Simulated contrasting influences  
475 of two La Niña Modoki events on aerosol concentrations over eastern China, *J.*  
476 *Geophys. Res. Atmos.*, 122, <https://doi.org/10.1002/2016JD026175>, 2017.

477 Gong, D. Y., Wang, S. W., and Zhu, J. H.: East Asian winter monsoon and Arctic  
478 Oscillation, *Geophys. Res. Lett.*, 28, 2073-2076,  
479 <https://doi.org/10.1029/2000GL012311>, 2001.

480 Hansen, J., Sato, M., and Ruedy, R.: Radiative forcing and climate response, *J. Geophys.*  
481 *Res.*, 102, D6, 6831-6864, <https://doi.org/10.1029/96JD03436>, 1997.

482 Harrison, D. E., and Larkin, N. K.: Seasonal U.S. temperature and precipitation  
483 anomalies associated with El Niño: Historical results and comparison with 1997-  
484 98, *Geophys. Res. Lett.*, 25, 3959–3962, <https://doi.org/10.1029/1998GL900061>,  
485 1998.

486 Hurrell, J. W.: Decadal trends in the North Atlantic Oscillation: Regional temperature  
487 and precipitation, *Science*, 269, 676-679, doi:10.1126/science.269.5224.676, 1995.

488 IPCC, *Climate change.: The physical science basis*. Cambridge University Press.  
489 Cambridge, UK, 2013.

490 Jeong, J. I., and Park, R. J.: Winter monsoon variability and its impacts on aerosol  
491 concentrations in East Asia, *Environ. Poll.*, 221, 285-292,

492 <https://doi.org/10.1016/j.envpol.2016.11.075>, 2017.

493 Jerez, S., Jimenez-Guerrero, P., Montavez, J. P., and Trigo, R. M.: Impact of the North  
494 Atlantic Oscillation on European aerosol ground levels through local processes: a  
495 seasonal model-based assessment using fixed anthropogenic emissions, *Atmos.*  
496 *Chem. Phys.*, 13, 11195-11207, <https://doi.org/10.5194/acp-13-11195-2013>, 2013.

497 Jiang, Y. Q., Yang, X. Q., Liu, X. H., Yang, D. J., Sun, X. G., Wang, M. H., Ding, A. J.,  
498 Wang, T. J., and Fu, C. B.: Anthropogenic aerosol effects on East Asian winter  
499 monsoon: The role of black carbon-induced Tibetan Plateau warming, *J. Geophys.*  
500 *Res. Atmos.*, 122, 5883-5902, <https://doi.org/10.1002/2016JD026237>, 2017.

501 Kalnay, E., Kanamitsu, M., Kistler, R., Colliins, W., Deaven, D., Gandin, L., Iredell,  
502 M., Saha, S., White, G., Woollen, J., Zhu, Y., Chelliah, M., Ebisuzaki, W., Higgins,  
503 W., Janowiak, J., Mo, K. C., Ropelewski, C., Wang, J., Leetmaa, A., Reynolds, R.,  
504 Jenne, R., and Joseph, D.: The NCEP/NCAR 40-Year Reanalysis Project, *Bull.*  
505 *Amer. Meteor. Soc.*, 77, 437-472, [https://doi.org/10.1175/1520-0477\(1996\)077<0437:TNYRP>2.0.CO;2](https://doi.org/10.1175/1520-0477(1996)077<0437:TNYRP>2.0.CO;2), 1996.

506

507 Karori, M. A., Li, J. P., and Jin, F. F.: The asymmetric influence of the two types of El  
508 Niño and La Niña on summer rainfall over southeast China, *J. Climate*, 26, 4567-  
509 4582, <https://doi.org/10.1175/JCLI-D-12-00324.1>, 2013.

510 Kleeman, M.: A preliminary assessment of the sensitivity of air quality in California to  
511 global change. *Climate Change*, 87, 273-292, <https://doi.org/10.1007/s10584-007-9351-3>, 2008.

512

513 Li, J. P., and Ruan, C. Q.: The North Atlantic–Eurasian teleconnection in summer and

514 its effects on Eurasian climates. *Environ. Res. Lett.*, 13,  
515 <https://doi.org/10.1088/1748-9326/aa9d33>, 2018.

516 Li, J. P., and Wang, J. X. L.: A new North Atlantic Oscillation index and its variability,  
517 *Adv. Atmos. Sci.*, 20, 661-676, <https://doi.org/10.1007/BF02915394>, 2003.

518 Li, K., Liao, H., Cai, W. J., and Yang, Y.: Attribution of anthropogenic influence on  
519 atmospheric patterns conducive to recent most severe haze over eastern China,  
520 *Geophys. Res. Lett.*, 45, 2072-2081, <https://doi.org/10.1002/2017GL076570>,  
521 2018.

522 Li, Y., Ma, B. S., Feng, J., and Lu, Y.: Influence of the strongest central Pacific ENSO  
523 events on the precipitation in eastern China, *Int. J. Climatol.*,  
524 <https://doi.org/10.1002/joc.6004>, 2019.

525 Liao, H., Henze, D. K., Seinfeld, J. H., Wu, S. L., and Mickley, L. J.: Biogenic  
526 secondary organic aerosol over the United States: Comparison of climatological  
527 simulations with observations, *J. Geophys. Res.*, 112,  
528 <https://doi.org/10.1029/2006JD007813>, 2007.

529 Liao, H., Chang, W., and Yang, Y.: Climatic effects of air pollutants over China: A  
530 review, *Adv. Atmos. Sci.*, 32, 115-139, doi:10.1007/s00376-014-0013-x, 2015.

531 Liu, H., Jacob, D. J., Bey, I., and Yantosca, R. M.: Constraints from <sup>210</sup>Pb and <sup>7</sup>Be on  
532 wet deposition and transport in a global three-dimensional chemical tracer model  
533 driven by assimilated meteorological fields, *J. Geophys. Res.*, 106, 12109-12128,  
534 <https://doi.org/10.1029/2000JD900839>, 2001.

535 Lou, S. J., Russell, L. M., Yang, Y., Xu, L., Lamjiri, M. A., DeFlorio, M. J., Miller, A.

536 J., Ghan, S. J., Liu, Y., and Singh, B.: Impacts of the East Asian monsoon on  
537 springtime dust concentrations over China, *J. Geophys. Res. Atmos.*, 121, 8137-  
538 8152, <https://doi.org/10.1002/2016JD024758>, 2016.

539 Lou, S. J., Yang, Y., Wang, H. L., Smith, S. J., Qian, Y., Rasch, P. J.: Black carbon amplifies  
540 haze over the North China Plain by weakening the East Asian winter monsoon, *Geophys.*  
541 *Res. Lett.*, 45, <https://doi.org/10.1029/2018GL080941>, 2018.

542 Mao, Y. H., Liao, H., and Chen H. S.: Impacts of East Asian summer and winter  
543 monsoons on interannual variations of mass concentrations and direct radiative  
544 forcing of black carbon over eastern China, *Atmos. Chem. Phys.*, 17, 4799-4816,  
545 <https://doi.org/10.5194/acp-17-4799-2017>, 2017.

546 Marshall, J., Johnson, H., and Goodman, J.: A study of the interaction of the North  
547 Atlantic Oscillation with ocean circulation, *J. Climate*, 14, 1399–1421,  
548 [https://doi.org/10.1175/1520-0442\(2001\)014<1399:ASOTIO>2.0.CO;2](https://doi.org/10.1175/1520-0442(2001)014<1399:ASOTIO>2.0.CO;2), 2001.

549 Moulin, C., Lambert, C. E., Dulac, F., and Dayan, U.: Control of atmospheric export of  
550 dust from North Atlantic by the North Atlantic Oscillation, *Nature*, 387, 691-694,  
551 <https://doi.org/10.1038/42679>, 1997.

552 Park, R. J., Jacob, D. J., Chin, M., and Martin, R. V.: Sources of carbonaceous aerosols  
553 over the United States and implications for natural visibility, *J. Geophys. Res.*, 108,  
554 4355, <https://doi.org/10.1029/2002JD003190>, 2003.

555 Park, R. J., Jacob, D. J., Field, B. D., Yantosca, R. M., and Chin, M.: Natural and  
556 transboundary pollution influences on sulfate-nitrate-ammonium aerosols in the  
557 United States: implications for policy, *J. Geophys. Res.*, 109, D15204,

558 <https://doi.org/10.1029/2003JD004473>, 2004.

559 Park, R. J., Jacob, D. J., Kumar, N., and Yantosca, R. M.: Regional visibility statistics  
560 in the United States: natural and transboundary pollution influences, and  
561 implications for the regional haze rule, *Atmos. Environ.*, 40, 5405-5423,  
562 <https://doi.org/10.1016/j.atmosenv.2006.04.059>, 2006.

563 Qin, Y., Chan, C. K., and Chan, L. Y.: Characteristics of chemical compositions of  
564 atmospheric aerosols in Hongkong: spatial and seasonal distributions, *Science of  
565 the total Environment*, 206, 25-37, [https://doi.org/10.1016/S0048-9697\(97\)00214-](https://doi.org/10.1016/S0048-9697(97)00214-3)  
566 [3](https://doi.org/10.1016/S0048-9697(97)00214-3), 1997.

567 Qiu, Y. L., Liao, H., Zhang, R. J., and Hu, J. L.: Simulated impacts of direct radiative  
568 effects of scattering and absorbing aerosols on surface-layer aerosol concentrations  
569 in China during a heavily polluted event in February 2014, *J. Geophys. Res.*, 122,  
570 5955-5975, <https://doi.org/10.1002/2016JD026309>, 2017.

571 Rasmusson, E. M., and Carpenter, T. H.: Variations in tropical sea surface temperature  
572 and surface wind fields associated with the Southern Oscillation/El Niño, *Mon.  
573 Wea. Rev.*, 110, 354-384, [https://doi.org/10.1175/1520-](https://doi.org/10.1175/1520-0493(1982)110<0354:VITSST>2.0.CO;2)  
574 [0493\(1982\)110<0354:VITSST>2.0.CO;2](https://doi.org/10.1175/1520-0493(1982)110<0354:VITSST>2.0.CO;2), 1982.

575 Rayner, N. A., Parker, D. E., Horton, E. B., Folland, C. K., Alexander, L. V., and Rowell,  
576 D. P.: Global analyses of sea surface temperature, sea ice, and night marine air  
577 temperature since the late nineteenth century, *J. Geophys. Res.*, 108, D14, 4407,  
578 <https://doi.org/10.1029/2002JD002670>, 2003.

579 Ropelewski, C. F., and Halpert, M. S.: Global and regional scale precipitation patterns

580 associated with the El Niño/Southern Oscillation, *Mon. Wea. Rev.*, 115, 1606-  
581 1626, [http://dx.doi.org/10.1175/1520-0493\(1987\)115<1606:GARSPP>2.0.CO;2](http://dx.doi.org/10.1175/1520-0493(1987)115<1606:GARSPP>2.0.CO;2),  
582 1987.

583 Singh, A., and Palazoglu, A.: Climatic variability and its influence on ozone and PM  
584 pollution in 6 non-attainment regions in the United States, *Atmos. Environ.*, 51,  
585 212–224, doi:10.1016/j.atmosenv.2012.01.020, 2012.

586 Trenberth, K. E.: The definition of El Niño, *Bull. Amer. Meteor. Soc.*, 78, 2771-2777,  
587 [https://doi.org/10.1175/1520-0477\(1997\)078<2771:TDOENO>2.0.CO;2](https://doi.org/10.1175/1520-0477(1997)078<2771:TDOENO>2.0.CO;2), 1997.

588 Visbeck, M. H., Hurrell, J. W., Polvani, L., and Cullen, H. M.: The North Atlantic  
589 Oscillation: past, present, and future, *PNAS*, 98, 12876-12877,  
590 <https://doi.org/10.1073/pnas.231391598>, 2001.

591 Wang, B., Wu, R. G., and Fu, X. H.: Pacific–East Asian teleconnection: how does  
592 ENSO affect East Asian Climate? *J. Climate*, 13, 1517-1536,  
593 [https://doi.org/10.1175/1520-0442\(2000\)013<1517:PEATHD>2.0.CO;2](https://doi.org/10.1175/1520-0442(2000)013<1517:PEATHD>2.0.CO;2), 2000.

594 Wang, Y. H., Jacob, D. J., and Logan, J. A.: Global simulation of tropospheric O<sub>3</sub>-NO  
595 x-hydrocarbon chemistry 1. model formulation, *J. Geophys. Res.*, 103, 10713,  
596 <https://doi.org/10.1029/98JD00158>, 1998.

597 Watanabe, M., and Nitta, T.: Decadal changes in the atmospheric circulation and  
598 associated surface climate variations in the Northern Hemisphere winter, *J. Climate*,  
599 12, 494-509, [https://doi.org/10.1175/1520-0442\(1999\)012<0494:DCITAC>2.0.CO;2](https://doi.org/10.1175/1520-0442(1999)012<0494:DCITAC>2.0.CO;2), 1999.

601 Weng, H. Y., Behera, S. K., and Yamagata, T.: Anomalous winter climate conditions in

602 the Pacific rim during recent El Niño Modoki and El Niño events, *Clim. Dyn.*, 32,  
603 663-674, <https://doi.org/10.1007/s00382-008-0394-6>, 2009.

604 Wesely, M. L.: Parameterization of surface resistances to gaseous dry deposition in  
605 regional-scale numerical models, *Atmos. Environ.*, 23, 1293-1304,  
606 [https://doi.org/10.1016/0004-6981\(89\)90153-4](https://doi.org/10.1016/0004-6981(89)90153-4), 1989.

607 Wu, J., and Wu, Z. W.: Interdecadal change of the spring NAO impact on the summer  
608 Pamir-Tianshan snow cover, *Int. J. Climatol.*, 39, 629-642,  
609 <https://doi.org/10.1002/joc.5831>, 2018.

610 Wu, R. G.: Seasonal dependence of factors for year-to-year variations of South China  
611 aerosol optical depth and Hong Kong air quality, *Int. J. Climatol.*, 34, 3204-3220,  
612 doi:10.1002/joc.3905, 2014.

613 Wu, Z. W., Wang, B., Li, J. P., and Jin, F.-F.: An empirical seasonal prediction model of  
614 the east Asian summer monsoon using ENSO and NAO, *J. Geophys. Res.*, 114,  
615 D18120, <https://doi.org/10.1029/2009JD011733>, 2009.

616 Wu, Z. W., Li, J. P., Jiang, Z. H., He, J. H., and Zhu, X. Y.: Possible effects of the North  
617 Atlantic Oscillation on the strengthening relationship between the East Asian  
618 summer monsoon and ENSO, *Int. J. Climatol.*, 32, 794-800,  
619 <https://doi.org/10.1002/joc.2309>, 2012.

620 Wu, Z. W., and Lin, H.: Interdecadal variability of the ENSO-North Atlantic Oscillation  
621 connection in boreal summer, *Q. J. Roy. Meteor. Soc.*, 138, 1668-1675,  
622 <https://doi.org/10.1007/s00382-014-2361-8>, 2012.

623 Wu, Z. W., Li, J. P., Jiang, Z. H., and He, J. H.: Predictable climate dynamics of

624 abnormal East Asian winter monsoon: once-in-a-century snowstorms in  
625 2007/2008 winter, *Clim. Dyn.*, 37, 1661-1669, [https://doi.org/10.1007/s00382-](https://doi.org/10.1007/s00382-010-0938-4)  
626 [010-0938-4](https://doi.org/10.1007/s00382-010-0938-4), 2011.

627 Wu, Z. W., and Zhang, P.: Interdecadal variability of the mega-ENSO-NAO  
628 synchronization in winter, *Clim. Dyn.*, 45, 1117-1128,  
629 <https://doi.org/10.1007/s00382-014-2361-8>, 2015.

630 Xie, S. P.: Satellite observations of cool ocean–atmosphere interaction, *Bull. Amer.*  
631 *Meteor. Soc.*, 85, 195-208, <https://doi.org/10.1175/BAMS-85-2-195>, 2004.

632 Xu, H. L., Feng, J., and Sun, C.: Impact of preceding summer North Atlantic Oscillation  
633 on early autumn precipitation over central China, *Atmos. Oceanic Sci. Lett.*, 6, 417-  
634 422, <https://doi.org/10.3878/j.issn.1674-2834.13.0027>, 2013.

635 Xuan, J., Liu, G. L., and Du, K.: Dust emission inventory in northern China, *Atmos.*  
636 *Environ.*, 34, 4565–4570, [https://doi.org/10.1016/S1352-2310\(00\)00203-X](https://doi.org/10.1016/S1352-2310(00)00203-X), 2000.

637 Yang, Y., Liao, H., Li, J.: Impacts of the East Asian summer monsoon on interannual  
638 variations of summertime surface-layer ozone concentrations over China, *Atmos.*  
639 *Chem. Phys.*, 14, 6867-6879, <https://doi.org/10.5194/acp-14-6867-2014>, 2014.

640 Yang, Y., Liao, H., and Lou, S. J.: Increase in winter haze over eastern China in the past  
641 decades: Roles of variations in meteorological parameters and anthropogenic  
642 emissions, *J. Geophys. Res. Atmos.*, 121, 13050-13065,  
643 <https://doi.org/10.1002/2016JD025136>, 2016.

644 Yang, Y., Russell, L. R., Lou, S. J., Liao, H., Guo, J. P., Liu, Y., Singh, B., and Ghan, S.  
645 J.: Dust-wind interactions can intensify aerosol pollution over eastern China,

646 Nature Comm., 8, 15333, <https://doi.org/10.1038/ncomms15333>, 2017.

647 Ye, X., and Wu, Z. W.: Contrasting impacts of ENSO on the interannual variations of  
648 summer runoff between the upper and mid-lower reaches of the Yangtze river,  
649 Atmosphere, 9, 478, <https://doi.org/10.3390/atmos9120478>, 2018.

650 Yue, X., and Unger, N.: Aerosol optical depth thresholds as a tool to assess diffuse  
651 radiation fertilization of the land carbon uptake in China, Atmos. Chem. Phys., 17,  
652 1329-1342, <https://doi.org/10.5194/acp-17-1329-2017>, 2017.

653 Zhang, L., Liao, H., and Li, J. P.: Impacts of Asian summer monsoon on seasonal and  
654 interannual variations of aerosols over eastern China, J. Geophys. Res., 115,  
655 D00K05, <https://doi.org/10.1029/2009JD012299>, 2010.

656 Zhang, P., Wang, B., and Wu, Z. W.: Weak El Niño and winter climate in the mid-high  
657 latitude Eurasia, J. Climate, 32, 402-421, [https://doi.org/10.1175/JCLI-D-17-](https://doi.org/10.1175/JCLI-D-17-0583.1)  
658 [0583.1](https://doi.org/10.1175/JCLI-D-17-0583.1), 2019a.

659 Zhang, P., Wu, Z. W., and Li, J. P.: Reexamining the relationship of La Niña and the  
660 East Asian winter monsoon, Clim. Dyn., [https://doi.org/10.1007/s00382-019-](https://doi.org/10.1007/s00382-019-04613-7)  
661 [04613-7](https://doi.org/10.1007/s00382-019-04613-7), 2019b.

662 Zhang, P., Wu, Z. W., and Chen H.: Interdecadal modulation of mega-ENSO on the  
663 north Pacific atmospheric circulation in winter, Atmos. Ocean, 55, 110-120,  
664 <https://doi.org/10.1080/07055900.2017.1291411>, 2017.

665 Zhang, R., Sumi, A., and Kimoto, M.: Impact of El Niño on the East Asian monsoon:  
666 A Diagnostic Study of the '86/87' and '91/92' events, J. Meteorol. Soc. Jpn., 74,  
667 49–62, [https://doi.org/10.2151/jmsj1965.74.1\\_49](https://doi.org/10.2151/jmsj1965.74.1_49), 1996. Zhang, R. H., Sumi, A.,

668 and Kimoto, M.: A diagnostic study of the impact of El Niño on the precipitation  
669 in China, *Adv. Atmos. Sci.*, 16, 229-241, <https://doi.org/10.1007/BF02973084>,  
670 1999.

671 Zhang, W. J., Wang, L., Xiang, B. Q., He, J. H.: Impacts of two types of La Niña on the  
672 NAO during boreal winter, *Clim. Dyn.*, 44, 1351-1366,  
673 <https://doi.org/10.1007/s00382-014-2155-z>, 2015.

674 Zhang, W. J., Mei, X. B., Geng, X., Turner, A. G., and Jin, F.-F.: A nonstationary ENSO-  
675 NAO relationship due to AMO modulation, *J. Climate*, 32, 33-43,  
676 <https://doi.org/10.1175/JCLI-D-18-0365.1>, 2019.

677 Zheng, F., Li, J. P., Li, Y. J., Zhao, S., and Deng, D. F.: Influence of the Summer NAO  
678 on the Spring-NAO-Based Predictability of the East Asian Summer Monsoon, *J.*  
679 *App. Meteorol. Climatol.*, 55, <https://doi.org/10.1175/JAMC-D-15-0199.1>, 2016.

680 Zhu, J. L., Liao, H., and Li, J. P.: Increases in aerosol concentrations over eastern China  
681 due to the decadal-scale weakening of the East Asian summer monsoon, *Geophys.*  
682 *Res. Lett.*, 39(9), L09809, <https://doi.org/10.1029/2012GL051428>, 2012.

683 Zuo, J. Q., Li, W. J., Sun, C. H., Xu, L., and Ren, H. L.: Impact of the North Atlantic  
684 sea surface temperature tripole on the East Asian summer monsoon, *Adv. Atmos.*  
685 *Sci.*, 30, 1173-1186, <https://doi.org/10.1007/s00376-012-2125-5>, 2013.

686

687 **Figure Captions:**

688 **Figure 1.** (a) The time series of the Niño3 index based on the GEOS-4 input skin  
689 temperature data for 1986-2006 ( $^{\circ}\text{C}$ ). (b) is similar to (a) but is based on the  
690 HadISST. (c) The time series of the NAO index based on the GEOS-4 input sea  
691 level pressure. (d) is similar to (c) but is based on the NCEP/NCAR reanalysis.

692 **Figure 2.** The standard deviation of the simulated (a) surface layer  $\text{PM}_{2.5}$  concentrations  
693 ( $\mu\text{g}\cdot\text{m}^{-3}$ ) and (b) column burdens of  $\text{PM}_{2.5}$  ( $\text{mg}\cdot\text{m}^{-2}$ ) during boreal winter averaged  
694 from 1986 to 2006. (c) The horizontal distribution of boreal winter climatological  
695 mean wind at 850 hPa ( $\text{m}\cdot\text{s}^{-1}$ ), shaded indicates the Tibetan Plateau.

696 **Figure 3.** (a) The spatial distribution of the correlation coefficients between surface  
697 layer  $\text{PM}_{2.5}$  concentrations and the Niño3 index. (b) As in (a), but for the  
698 correlations with the NAOI. Color shading indicates a significant correlation at the  
699 0.1 level (0.37 is the critical value for significance at the 0.1 level).

700 **Figure 4.** Spatial distribution of the correlation coefficients between (a) positive and (b)  
701 negative Niño3 index values and surface-layer  $\text{PM}_{2.5}$  concentrations. (c)-(d) as in  
702 (a)-(b), but for the NAOI. Color shading indicates a significant correlation, (0.35  
703 and 0.45 are the critical value for significance at the 0.2 and 0.1 level, respectively).

704 **Figure 5.** The spatial distribution of the simulated anomalous (left panel) surface layer  
705  $\text{PM}_{2.5}$  concentrations ( $\mu\text{g}\cdot\text{m}^{-3}$ ) and (right panel) column burdens of  $\text{PM}_{2.5}$  ( $\text{mg}\cdot\text{m}^{-2}$ )  
706 during the boreal winters of 1997 (upper) and 2002 (below).

707 **Figure 6.** The pressure–latitude distribution of zonally averaged  $\text{PM}_{2.5}$  anomalies over  
708  $105^{\circ}$ – $120^{\circ}\text{E}$  during the winters of (a)1997 and 2002 ( $\mu\text{g}\cdot\text{m}^{-3}$ ).

709 **Figure 7.** The horizontal distribution of surface wind ( $\text{m}\cdot\text{s}^{-1}$ ) and surface level pressure  
710 (hPa) based on the assimilated meteorological data during the autumns of (a) 1997  
711 and (b) 2002.

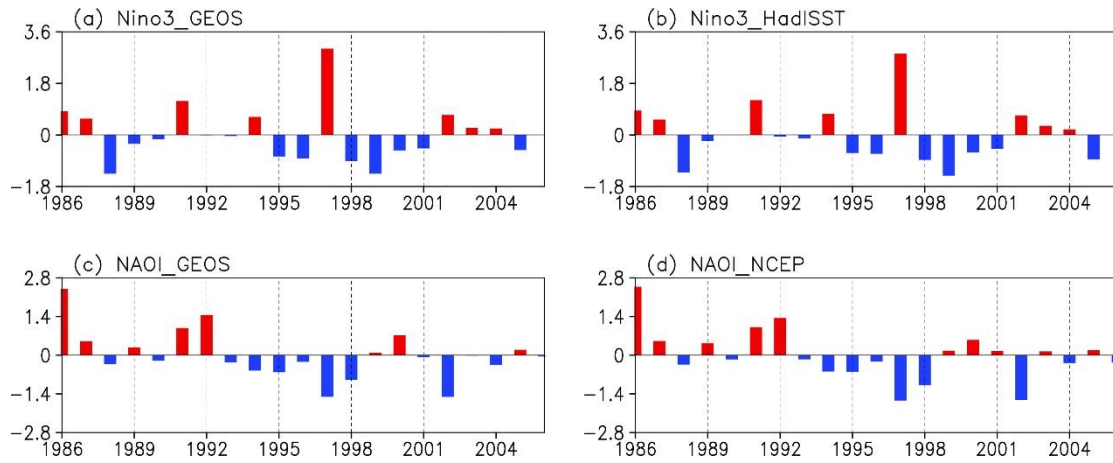
712 **Figure 8.** The horizontal distribution of skin temperature anomalies ( $^{\circ}\text{C}$ ) based on the  
713 assimilated meteorological data during the (a) autumn and (b) winter of 1997. (c)-  
714 (d) As in (a)-(b), but during 2002.

715 **Figure 9.** Horizontal distribution of the divergence ( $10^{-5}\text{s}^{-1}$ ) at 300 hPa during the  
716 winters of (a) 1997 and (b) 2002. The crosses denote the centers of action of the  
717 AEA pattern.

718 **Figure 10.** Horizontal distribution of 850 hPa wind anomalies (vectors;  $\text{m}\text{ s}^{-1}$ ) and  
719 divergence (shading;  $10^{-5}\text{s}^{-1}$ ) at 700 hPa during the winters of (a) 1997 and (b)  
720 2002.

721 **Figure 11.** The spatial distribution of the vertically integrated wet deposition flux  
722 anomalies during the winters of (a) 1997 and (b) 2002. (c)-(d), As in (a)-(b), but  
723 for the anomalous distribution of aerosol concentrations when the wet deposit is  
724 turned off.

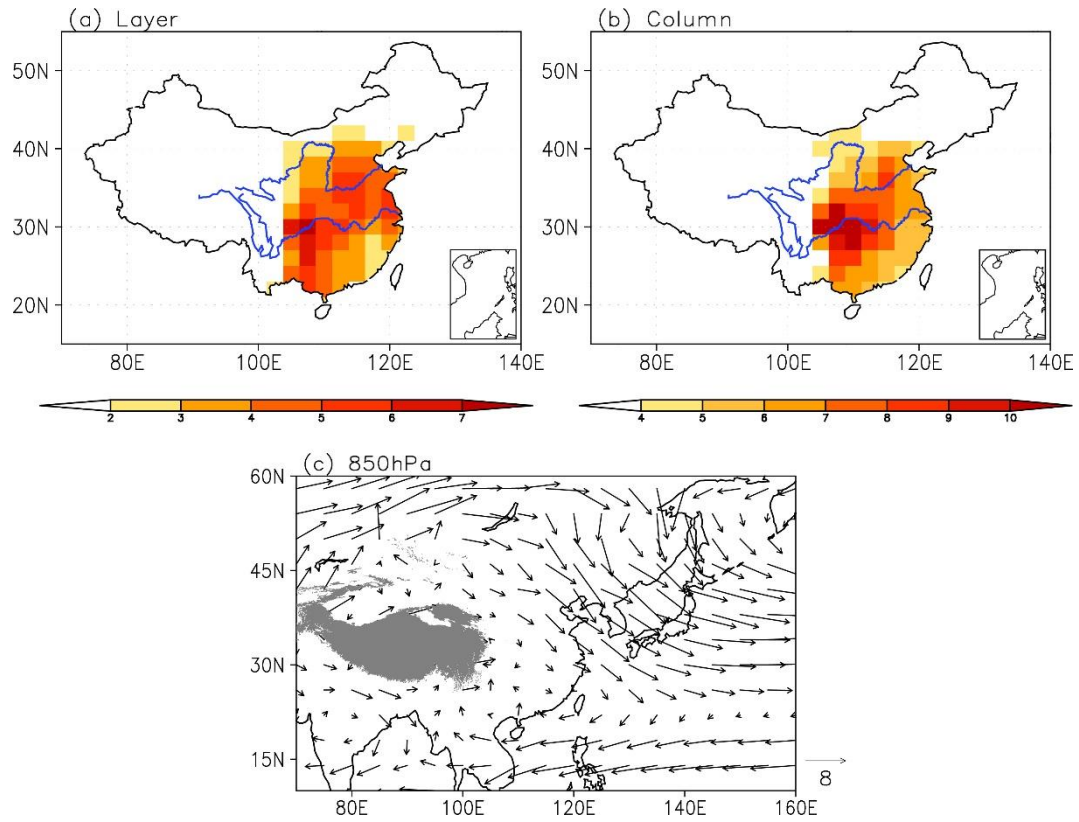
725



726

727 **Figure 1.** (a) The time series of the Niño3 index based on the GEOS-4 input skin  
 728 temperature data for 1986-2006 (°C). (b) is similar to (a) but is based on the HadISST.  
 729 (c) The time series of the NAO index based on the GEOS-4 input sea level pressure. (d)  
 730 is similar to (c) but is based on the NCEP/NCAR reanalysis.

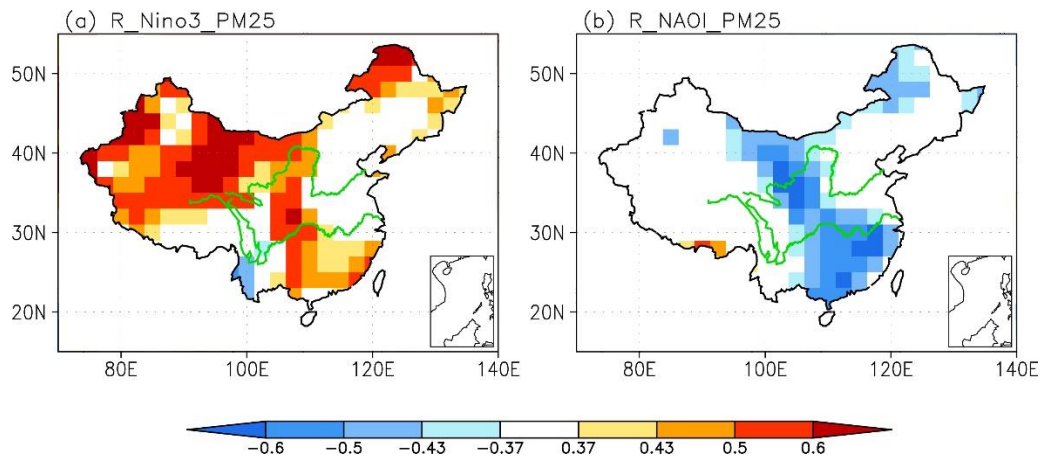
731



732

733 **Figure 2.** The standard deviation of the simulated (a) surface layer PM<sub>2.5</sub> concentrations  
 734 ( $\mu\text{g}\cdot\text{m}^{-3}$ ) and (b) column burdens of PM<sub>2.5</sub> ( $\text{mg}\cdot\text{m}^{-2}$ ) during boreal winter averaged from  
 735 1986 to 2006. (c) The horizontal distribution of boreal winter climatological mean wind  
 736 at 850 hPa ( $\text{m}\cdot\text{s}^{-1}$ ), shaded indicates the Tibetan Plateau.

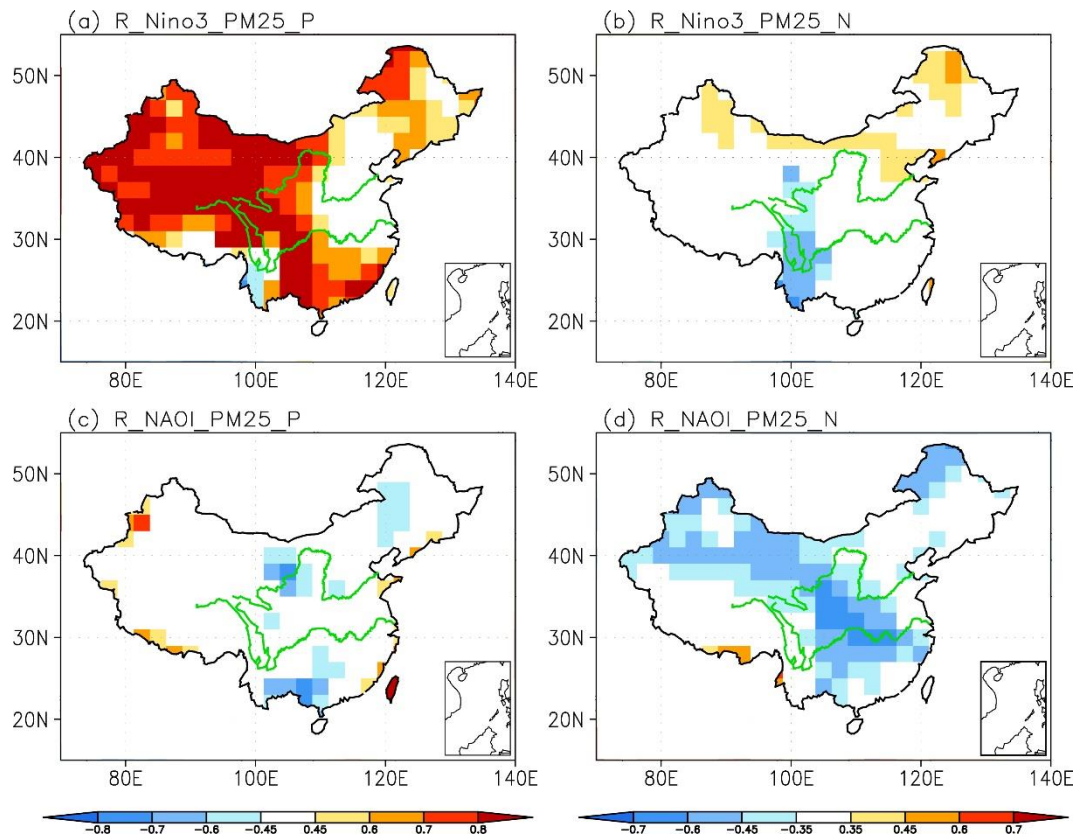
737



738

739 **Figure 3.** (a) The spatial distribution of the correlation coefficients between surface  
 740 layer PM<sub>2.5</sub> concentrations and the Niño3 index. (b) As in (a), but for the correlations  
 741 with the NAOI. Color shading indicates a significant correlation at the 0.1 level (0.37  
 742 is the critical value for significance at the 0.1 level).

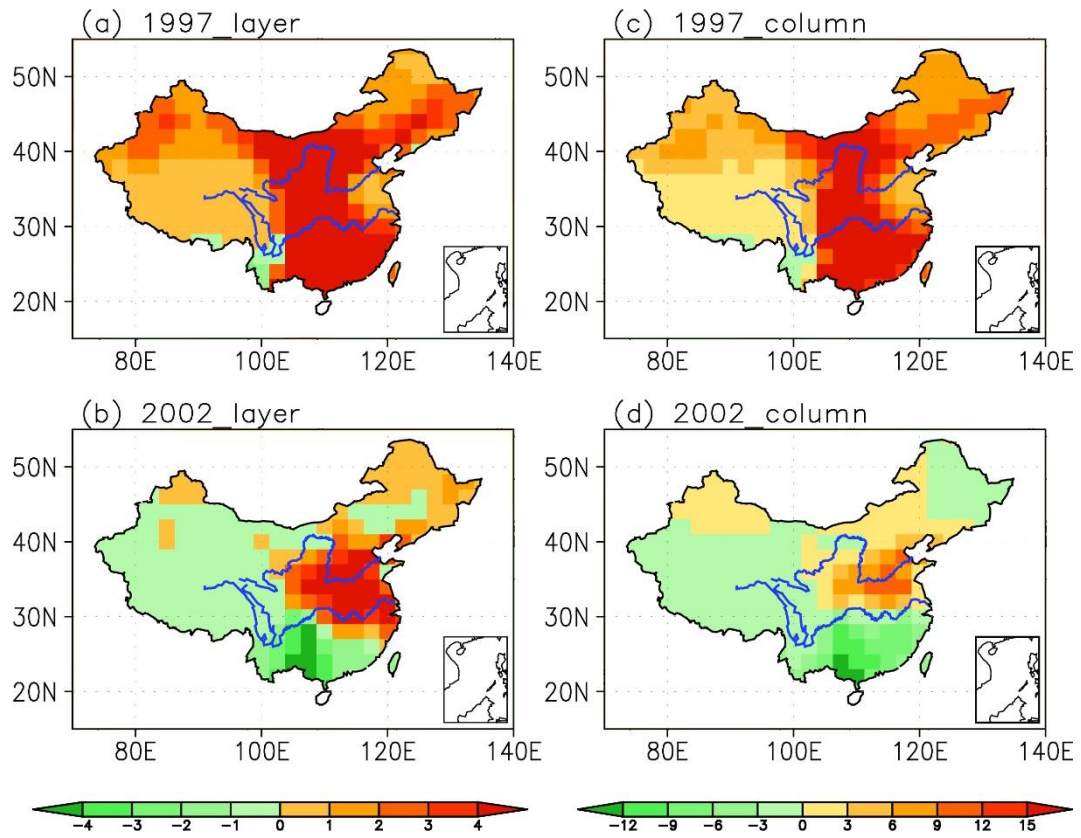
743



744

745 **Figure 4.** Spatial distribution of the correlation coefficients between (a) positive and (b)  
 746 negative Niño3 index values and surface-layer PM<sub>2.5</sub> concentrations. (c)-(d) as in (a)-  
 747 (b), but for the NAOI. Color shading indicates a significant correlation, (0.35 and 0.45  
 748 are the critical value for significance at the 0.2 and 0.1 level, respectively).

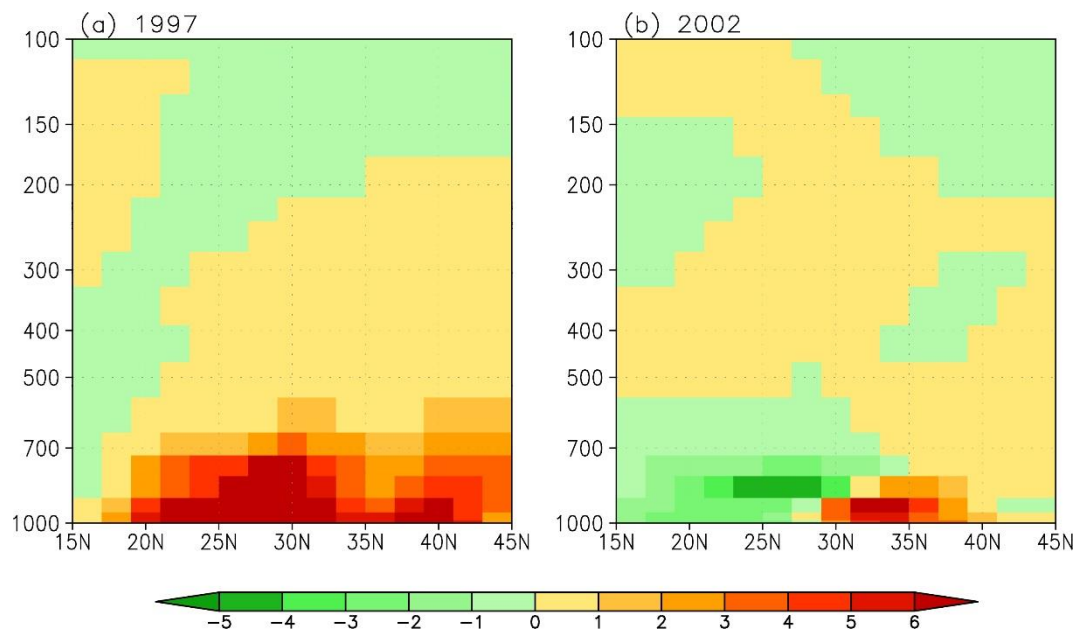
749



750

751 **Figure 5.** The spatial distribution of the simulated (left panel) anomalous surface layer  
 752 PM<sub>2.5</sub> concentrations ( $\mu\text{g}\cdot\text{m}^{-3}$ ) and (right panel) column burdens of PM<sub>2.5</sub> ( $\text{mg}\cdot\text{m}^{-2}$ )  
 753 during the boreal winters of 1997 (upper) and 2002 (below).

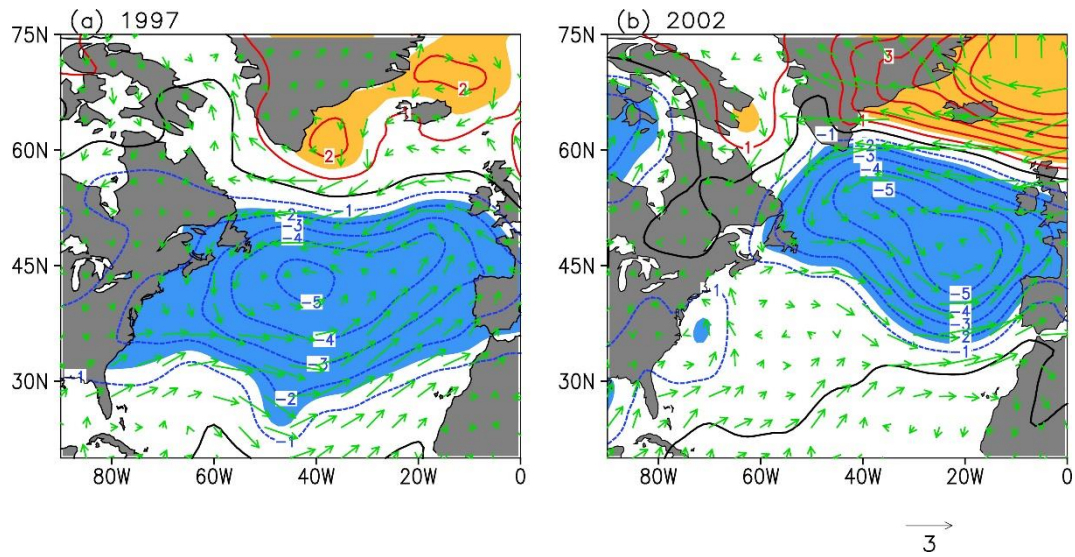
754



755

756 **Figure 6.** The pressure–latitude distribution of zonally averaged PM<sub>2.5</sub> anomalies over  
 757 105°–120°E during the winters of (a)1997 and 2002 ( $\mu\text{g}\cdot\text{m}^{-3}$ ).

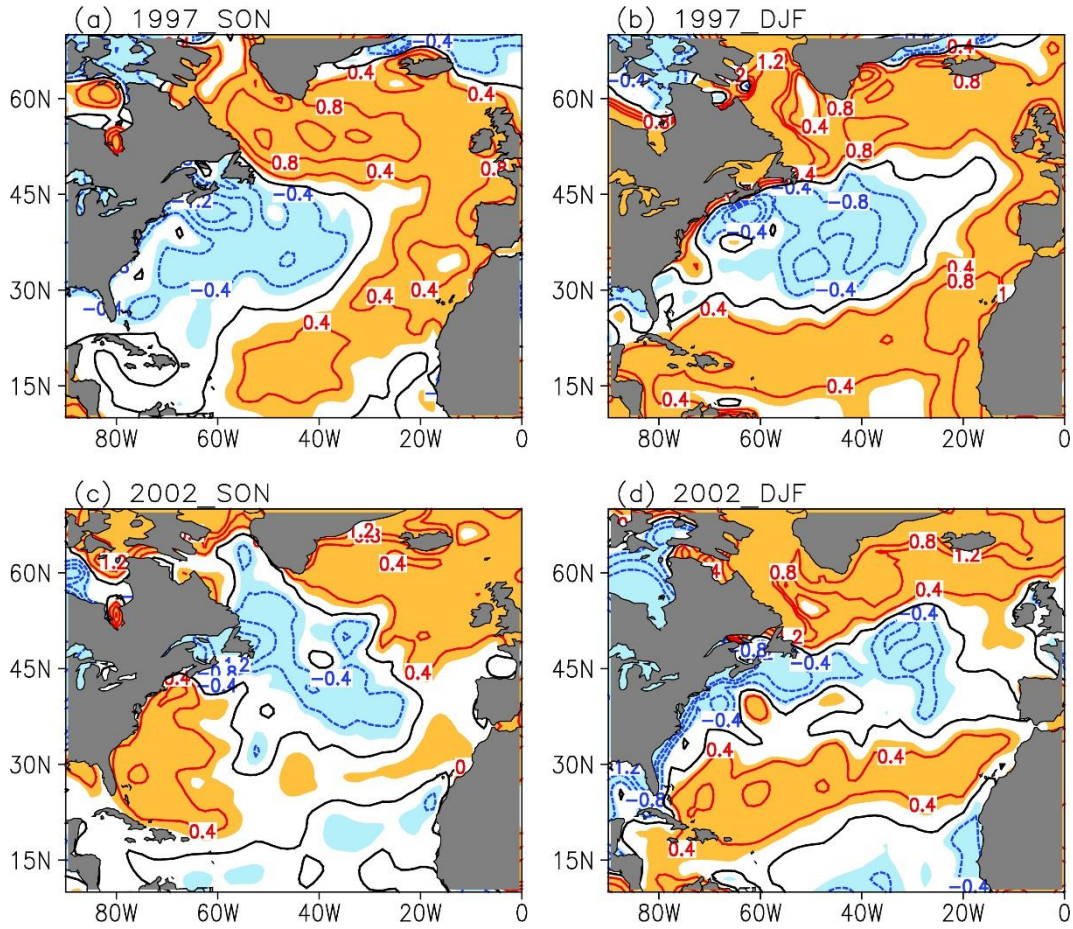
758



759

760 **Figure 7.** The horizontal distribution of surface wind ( $\text{m}\cdot\text{s}^{-1}$ ) and surface level pressure  
 761 (hPa) based on the assimilated meteorological data during the autumns of (a) 1997 and  
 762 (b) 2002.

763



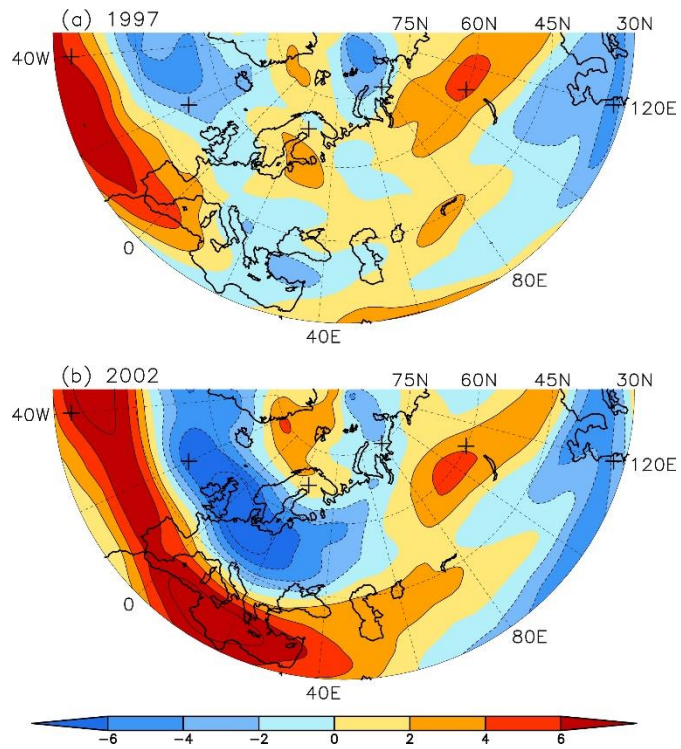
764

765 **Figure 8.** The horizontal distribution of skin temperature anomalies ( $^{\circ}\text{C}$ ) based on the

766 assimilated meteorological data during the (a) autumn and (b) winter of 1997. (c)-(d)

767 As in (a)-(b), but during 2002.

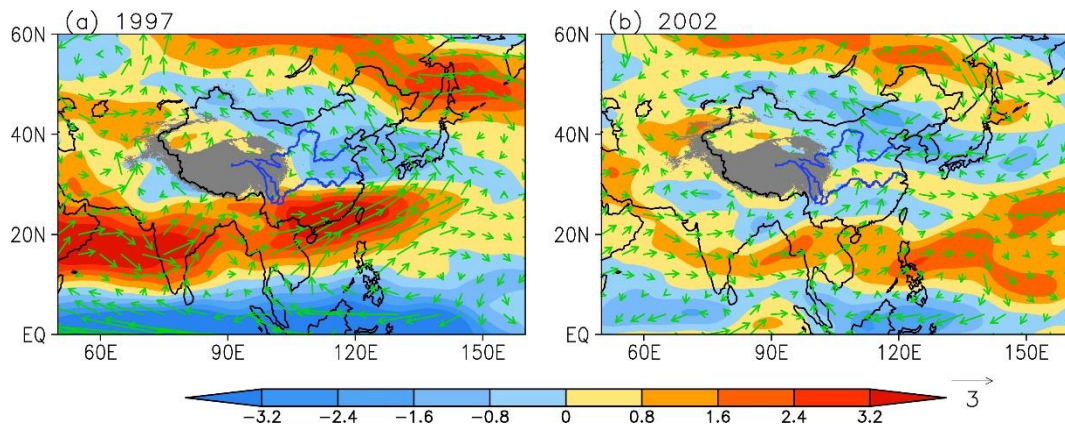
768



769

770 **Figure 9.** Horizontal distribution of the divergence ( $10^{-5} \text{s}^{-1}$ ) at 300 hPa during the  
 771 winters of (a) 1997 and (b) 2002. The crosses denote the centers of action of the AEA  
 772 pattern.

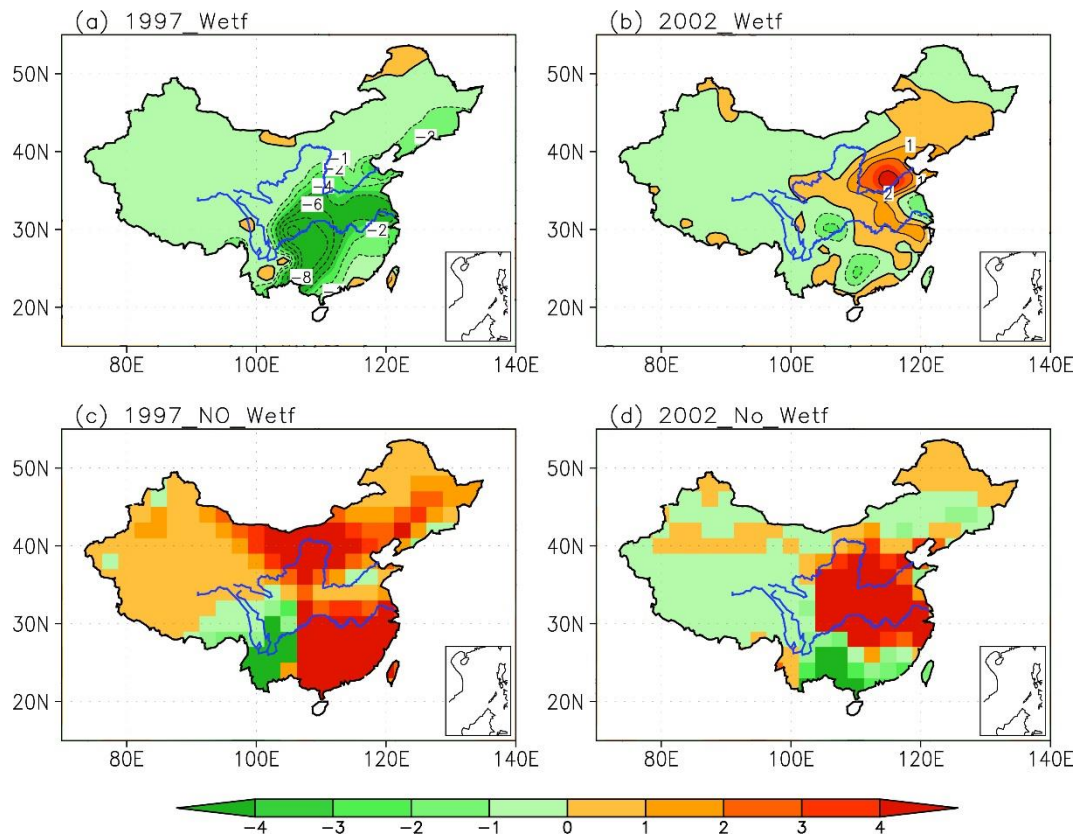
773



774

775 **Figure 10.** Horizontal distribution of 850 hPa wind anomalies (vectors;  $\text{m s}^{-1}$ ) and  
 776 divergence (shading;  $10^{-5}\text{s}^{-1}$ ) at 700 hPa during the winters of (a) 1997 and (b) 2002.

777



778

779 **Figure 11.** The spatial distribution of the vertically integrated wet deposition flux  
 780 anomalies during the winters of (a) 1997 and (b) 2002. (c)-(d), As in (a)-(b), but for the  
 781 anomalous distribution of aerosol concentrations when the wet deposit is turned off.